J. Synchrotron Rad. (1999). **6**, 370–372

XAFS studies of interfaces in MnSe/ZnTe superlattices

A. J. Kropf,[a] B. A. Bunker, J. K. Furdyna

Department of Physics, University of Notre Dame, Notre Dame, IN 46556, USA, [a]Present address: Chemical Technology Division, Argonne National Laboratory, Argonne, IL 60439, USA

Polarization-dependent XAFS measurements of a series of MnSe/ZnTe superlattices are presented. The results are consistent with a small interdiffusion at the interfaces, accompanied by an elastic distortion of the bond angles. This is in contrast to earlier measurements of other II-VI semiconductor superlattices. In addition, the Zn-Se bond expands by 0.027±0.012 Å to accommodate the strain in the superlattice.

Keywords: polarized XAFS; superlattice; interface.

1. Introduction

Polarization-dependent XAFS may be used as a sensitive probe of the interface of multi-layer materials. By varying the layer thickness and the thickness ratios, detailed information about the structure may be obtained. A number of such systems have been studied; one is CdSe/ZnTe, the first lattice-matched binary II-VI system to be grown as a superlattice with neither the anions nor the cations in common (Samarth et. al, 1990, Kemner et. al., 1993).

An XAFS study of the CdSe/ZnTe superlattice system was performed by Kemner et al. (1994a). This investigation, using XAFS and x-ray diffraction (XRD) techniques, presented results consistent with an exchange of entire planes of atoms across the interface; two layers of anions or cations would switch and then remain fixed as additional layers were deposited. This forms a high-strain structure at the interface due to the domination of the bond formation energy over the increased strain energy of the new arrangement.

Another quaternary system grown soon thereafter was a MnSe/ZnTe superlattice. While both MnSe and CdSe grow naturally in a wurtzite structure, by depositing Se with Mn or Cd atoms on the (100) surface of a zinc-blende crystal, it is possible to constrain the growth to a zinc-blende phase. This phase is stable up to a critical thickness that is much larger than the layer thickness used in this study. However, in contrast to the CdSe/ZnTe superlattice, the MnSe/ZnTe superlattice has a large lattice mismatch (~3%), leading to a highly strained structure (Yoder-Short et. al, 1985). In the MnSe/ZnTe system the strain energy is expected to be the dominant factor. This is a significant contrast with the CdSe/ZnTe superlattice system. The MnSe/ZnTe superlattice also exhibits a unique magnetic structure that may be understood in terms of the structure of the MnSe layers (Geibultowicz et. al, 1992a, Geibultowicz et. al, 1992b).

2. Experiment

The MnSe/ZnTe superlattices were prepared by MBE using a Riber 32 R&D system by the group of J. K. Furdyna at the University of Notre Dame. These superlattices were grown on a GaAs (100) substrate with a 1-3 μm ZnTe buffer layer to decrease the dislocation density due to the 7% lattice mismatch between the ZnTe and GaAs substrate. The sample preparation is described in more detail by Geibultowicz, et. al (1992b).

By growing a thick buffer layer, the superlattice will tend to follow the in-plane spacing of the ZnTe layer and consequently strain the MnSe layers, which have a smaller relaxed lattice. The samples studied consist of 74 to 300 repetitions of the following nominal MnSe/ZnTe bilayers: (3/3), (3/6), (5/11), (11/16) and (12/21). One bilayer of a (3/3) superlattice would consist of the following atomic layers (Mn-Se-Mn-Se-Mn-Se)-(Zn-Te-Zn-Te-Zn-Te). In this arrangement the number of Mn-Te bonds at one interface will equal the number of Zn-Se bonds at another interface. In addition, for a perfect arrangement of the (3/3) superlattice, the average number of Mn-Te bonds around the Mn atoms will also be equal to the average number of Zn-Se bonds around Zn atoms ($N_{\text{Mn-Te}}=N_{\text{Zn-Se}}=2/3$).

XAFS data were collected at the Mn, Zn, and Se K-edges (6538 eV, 9659 eV, and 12658 eV, respectively) using a specially designed detector for making simultaneous total electron yield (TEY) and fluorescence measurements at low temperature (~80 K) in any sample orientation with respect to the incident beam polarization. An earlier model of this low-temperature, TEY detector is described by Kemner, et. al. (1994b).

3. Data and Interpretation

Since superlattices are not isotropic, it is possible to use the incident x-ray polarization to look preferentially at either the atoms in the growth plane or perpendicular to the growth plane of the superlattice. This corresponds to looking at bonding in the layers and across the interface between layers, at least for thin layers. Differences will be seen in the first-shell amplitudes due to the $\cos^2\theta$ dependence of the XAFS on the polarization angle, while more dramatic differences in the second-shell distances should be observed because of the strain induced in the superlattice.

Similar measurements were made on epitaxially grown standards: MnTe for the Mn K-edge, ZnSe and ZnTe for the Zn

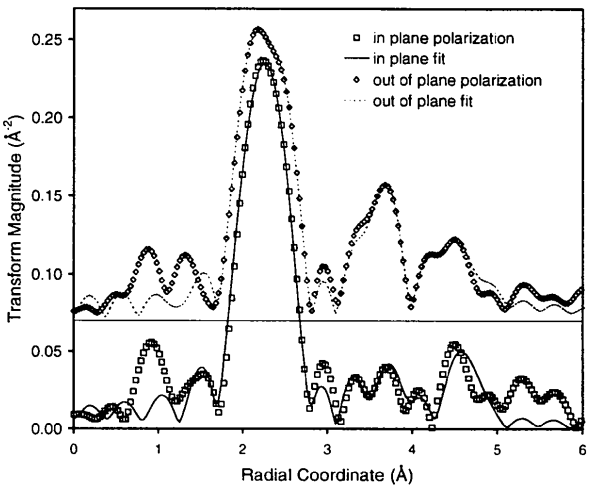

Figure 1
Fourier-transformed of Mn edge data for the (3/6) sample showing spectra obtained with the x-ray polarization both in-plane (open squares) and out-of-plane (open triangles) with three shell calculated fits (solid and dashed lines). (k-range 2.75-11.25 Å^{-1}, dk_1=0.25, dk_2=0.5, r-range 1.75-4.7 Å). Data offset by 0.07 Å^{-2} for clarity.

Table 1
Zn edge (top) and Mn edge (bottom) fitting results for the first shell for coordination number and radial distance. Total coordination was set to four. For the Zn edge, k-range 2.5-12.5 Å^{-1}, k^1 weighting, r-range 1.6-3.01 Å, dr=0.2 Å. For the Mn edge, k-space range 2.5-10.25 Å^{-1}, k^1 weighting, r-space range 1.6-2.9 Å, dr=0.2 Å. 'pll' and 'ppd' refer to the in-plane and out-of-plane polarization measurements, respectively.

Sample	$N_{Zn\text{-}Te}$	Zn-Te Radial Distance (Å)	$N_{Zn\text{-}Se}$	Zn-Se Radial Distance (Å)
Bulk ZnTe	4.0	2.642	-----	-----
Bulk ZnSe	-----	-----	4.0	2.455
3/3 - pll	2.68(0.15)	2.617(0.015)	1.32(0.15)	2.471(0.02)
3/3 - ppd	2.69(0.15)	2.615(0.015)	1.31(0.15)	2.474(0.02)
3/6 - pll	3.21(0.15)	2.641(0.01)	0.79(0.15)	2.503(0.02)
3/6 - ppd	3.18(0.15)	2.627(0.01)	0.82(0.15)	2.472(0.02)
12/21 - pll	3.66(0.20)	2.639(0.01)	0.34(0.20)	2.48(0.03)
12/21 - ppd	3.68(0.20)	2.639(0.01)	0.32(0.20)	2.49(0.03)
	$N_{Mn\text{-}Se}$	Mn-Se Radial Distance (Å)	$N_{Mn\text{-}Te}$	Mn-Te Radial Distance (Å)
Bulk MnSe	4.0	2.557	-----	-----
Bulk MnTe	-----	-----	4.0	2.745
3/3 - ppd	2.80(0.15)	2.548(0.015)	1.20(0.15)	2.746(0.02)
3/6 - pll	3.11(0.15)	2.574(0.015)	0.89(0.15)	2.745(0.02)
3/6 - ppd	2.84(0.15)	2.580(0.015)	1.16(0.15)	2.747(0.02)
5/11 - pll	3.57(0.20)	2.570(0.015)	0.43(0.20)	2.73(0.04)
5/11 - ppd	3.54(0.20)	2.570(0.015)	0.46(0.20)	2.70(0.04)
12/21 -pll	3.76(0.12)	2.560(0.010)	0.24(0.12)	2.74(0.06)

K-edge, and ZnSe for the Se K-edge. The first-shell data was analyzed primarily by direct comparison to the experimental standards. However, the higher-shell data were analyzed using the FEFF code (version 6.01) (Rehr et. al., 1991). The suitability of FEFF for this study was verified through modeling of the XAFS data from the epitaxially-grown thin films.

XAFS measurements at the Mn K-edge were obtained in both fluorescence and TEY modes. Fluorescence XAFS measurements were made using a 13-element solid-state detector tuned to the Mn K_α energy, in order to reduce the large background signal from the Te L-edges and elastically scattered photons.

At the Se K-edge, TEY and fluorescence measurements are both used. TEY measurements have a significantly better S/N and may be "deglitched" (from small Bragg diffraction contamination) by measuring the XAFS at a few slightly varying angles. Data from different orientations may be compared with the fluorescence data if there is any question as to which features are due to the XAFS and which are due to diffraction. The fluorescence measurements alone are inadequate because of the total count rate limitation of solid-state detectors and the large background signal from the GaAs substrate and ZnTe buffer layer: fluorescence x rays from both of which are excited by Se K-edge energy x rays.

To obtain complementary information to the Mn K-edge results, the Zn K-edge XAFS data were taken in the TEY mode. The TEY mode must be used to avoid contamination from the ZnTe buffer layer. The Zn K-edge Auger electron escape depth (Elam et. al., 1988) of ~1500 Å is less than the total superlattice thickness (always greater than 1850 Å), giving one the surface sensitivity required.

To illustrate the polarization dependence of the XAFS data, plots of $\tilde{\chi}(r)$ at the Mn edge are shown in Fig. 1. These spectra demonstrate the bending of the near-neighbor bonds into the growth plane of the superlattice, as evidenced by the larger in-plane amplitude versus the out-of-plane amplitude of the first shell. Similar results at the Zn K-edge show that the ZnTe layers are slightly expanded in the growth direction. Fitting the intensity of the XRD superlattice lines corroborates this result (Kropf, 1997).

For the Zn K-edge, the data are fairly easy to interpret. From the results, if there is a distortion due to the buffer layer, it is clearly very small. Two of the samples, (5/11) and (11/16), had thick ZnTe caps on the surface, making them unsuitable for this phase of the study. The results of fitting the isolated first shell data to experimental standards are shown in Table 1. An example of the inverse transformed data along with the resulting fit is shown in Fig. 2. It is evident that in addition to the bond angle distortion, the Zn-Se bond is stretching to accommodate the strain in the superlattice.

The results of fitting the Mn K-edge data are also shown in Table 1. In this case, since there was not a suitably characterized epitaxial MnSe standard available, the longest-period (12/21) sample was used as the experimental reference. The first shell of this sample was fit with theoretical scattering paths to determine as well as possible the contribution of Mn-Te bonds to the XAFS. This is shown in the last row of the table. The other data were fit using sample (12/21) as a standard, correcting the results for the small Mn-Te contribution present.

A few results should be highlighted. Except in the case of shortest period 3/3 superlattice, some expansion of the Mn-Se bond is occurring. Also, for the 3/6 superlattice there is a clear difference in $N_{Mn\text{-}Te}$ between the in-plane and out-of-plane polarizations. This due to the length of the Mn-Te bond: larger than the underlying lattice. These bonds will bend out of the growth plane and enhance the Mn-Te signal for the out-of-plane polarization measurements. A calculation based on the measured coordination numbers (considering that the relative error is smaller than the absolute error) and the MnSe layer lattice distortion (from the first shell amplitude) results in a 3.0±1.5° bending of the Mn-Te bond (across the interface) out of the growth plane relative to the tetrahedral bond angle. This is a determination separate from the expected bond bending due to the lattice mismatch between ZnTe and MnSe.

While the quality of the TEY data for the Se edge was very good in most cases, the Se-Mn and Se-Zn paths are nearly indistinguishable. Thus, independent measurements of the Zn-Se and Mn-Se path parameters are not available.

The measured coordination number vs. layer thickness, along with the predicted coordination number for two possible models, is shown in Fig. 3. Where there is a difference in the coordination number with polarization, an average is taken as the actual coordination number. If an interface was perfectly ordered, with an integral number of atomic monolayers per superlattice layer,

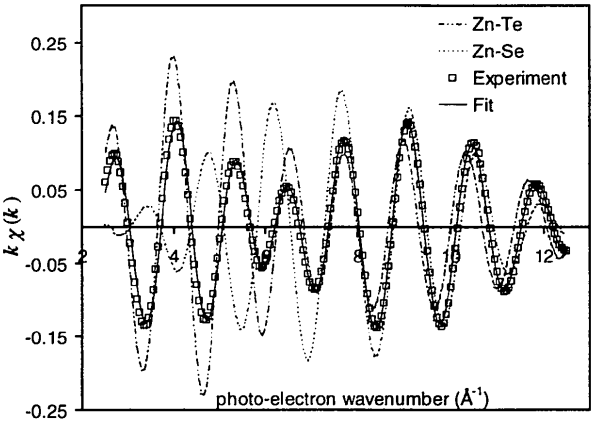

Figure 2
Example of fitting Fourier-filtered first-shell data of the (3/3) sample to experimental standards for the Zn edge. (room temperature, k-range 2.5-12.5 Å^{-1}, dk=0.5, k^1 weighting, r-range 1.6-3.01 Å, dr=0.2 Å.)

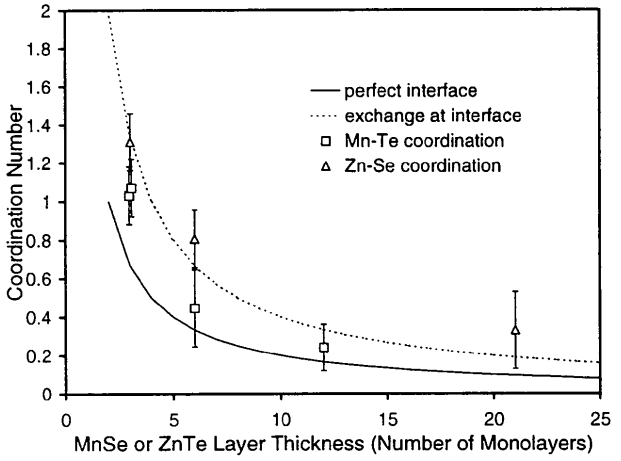

Figure 3

$N_{Mn\text{-}Te}$ ($N_{Zn\text{-}Se}$) vs. MnSe (ZnTe) layer thickness. The solid line depicts the minimum average value of $N_{Mn\text{-}Te}$ and $N_{Zn\text{-}Se}$ for a perfect interface, while the dotted line shows the expected value for plane exchange across the interface.

the solid line shows the minimum average coordination number possible: $(N_{Mn\text{-}Te}+N_{Zn\text{-}Se})/2$. If entire planes of atoms exchange across such an interface, the dotted line is the expected coordination number.

For either situation or for simple interdiffusion, $N_{Mn\text{-}Te}$ should equal $N_{Zn\text{-}Se}$ in layers of equal thickness. Since it is clear that $N_{Mn\text{-}Te}$ does not equal $N_{Zn\text{-}Se}$ for equal layer thickness, one of two possibilities exists for the ordering at the interface. The first is that Zn (or Se) atoms are substitutionally replacing Mn (or Te) atoms in the adjacent layer. The second possibility is that a ZnSe interface layer is preferred, while a MnTe interface layer is less likely. Given either of these models, interdiffusion also occurs, which increases the average coordination number above the value for a perfect interface.

The higher shell data (fitting results shown in Fig. 1) also show polarization dependence. The measurements taken in the out-of-plane polarization orientation only sample the second-shell paths in neighboring growth planes, while the in-plane measurements sample the second shell paths in the growth plane as well as those in neighboring planes. These effects are too small to detect around the Zn atoms, but the out-of-plane Mn XAFS shows a Mn-Mn distance contraction of 0.05±0.02 Å in the growth direction. In addition, these measurements show a Mn-Zn distance of 4.37±0.05 Å (an expansion of 0.2 Å) when measured across Te atoms at the interface and a Mn-Zn distance contraction of 0.10 Å measured across Se atoms at the interface. The in-plane Mn XAFS shows a Mn-Mn distance expansion of 0.08±0.04 Å. These results are from measurements on samples (3/6) and (5/11).

4. Summary and Conclusions

Using fluorescence and electron-yield detection, a series of MnSe/ZnTe superlattices has been investigated. The results indicate some interdiffusion, but this is accompanied by a more complex atomic replacement reaction, which appears as an asymmetry in the near-neighbor coordination number as a function of the layer thickness (Fig. 3). The XAFS data are not able to differentiate between the two possibilities. The first, a higher incidence of Zn-Se interfaces than Mn-Te interfaces. The second being a substitutional replacement of atoms on the surface by the deposition of the new layer. The effect of strain is also seen in these layers, and the bond-bending angle is determined from the experimental results. Analysis of the higher shell data shows that the XAFS is sensitive to bonds across the interface between layers.

We acknowledge the support of the U.S. Department of Energy (DOE), Division of Materials Research, Office of Basic Energy Sciences under Contract No. DE-FG05-89ER45384 for its role in the development and operation of the X-11 beam line at the National Synchrotron Light Source (NSLS) at Brookhaven National Laboratory. The X23-A2 beam line at the NSLS is supported in part by the National Institute of Standards and Technology. The NSLS is supported by the Department of Energy (Division of Materials Science and Division of Chemical Sciences of the Office of Basic Energy Sciences) under Contract No. DE-AC02-76CH00016.

References

Elam, W. T., Kirkland, J. P., Neiser, R. A., & Wolf, P. D. (1988), *Phys. Rev. B* **38**, 26-30.

Giebultowicz, T. M., Klosowski, P., Rhyne, J. J., Samarth, N., Luo, H., & Furdyna, J. K. (1992a), *Physica B* **180&181**, 485-488.

Giebultowicz, T. M., Samarth, N., Luo, H., Furdyna, J. K., Klosowski, P., & Rhyne, J. J. (1992b), *Phys. Rev. B* **46**, 12076.

Kemner, K. M., Bunker, B. A., Luo, H., Samarth, N., Furdyna, J. K., Weidmann, M. R., & Newman, K. E. (1993), *Proc. 7th Intl. Conf. X-ray Absorption Fine Structure, Kobe, 1992. Jpn. J. Appl. Phys.* **32**(2), 399-403.

Kemner, K. M., Bunker, B. A., Kropf, A. J., Luo, H., Samarth, N., Furdyna, J. K., Weidmann, M., & Newman, K. (1994a), *Phys. Rev. B* **50**, 14327-9.

Kemner, K. M., Bunker, B. A., & Kropf, A. J. (1994b), *Rev. Sci. Instrum.* **65**, 3667.

Kropf, A. J. (1997), *PhD dissertation*, University of Notre Dame, USA.

Rehr, J. J., Mustre DeLeon, J., & Zabinsky, S. I. (1991), *J. Am. Chem Soc.* **113**, 5135.

Samarth, N., Luo, H., Furdyna, J. K., Lee, Y. R., Alonso, R. G., Smith, E. K., Ramdas, A. K., & Otsuka, N. (1990), *Surf. Sci.* **228**, 226.

Yoder-Short, D. R., Debska, U., & Furdyna, J. K. (1995), *J. Appl. Phys.* **58**, 4056.

(Received 10 August 1998; accepted 28 January 1999)